

# Compression Behaviors of Binary Skutterudite $\text{CoP}_3$ in Noble Gases up to 40 GPa at Room Temperature

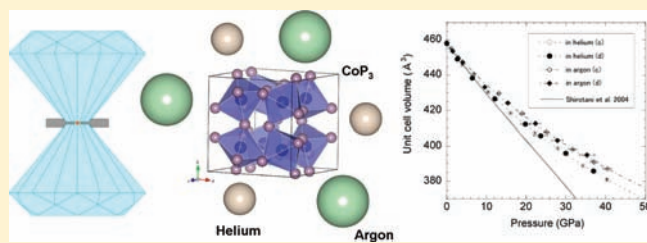
Ken Niwa,<sup>\*,†</sup> Daisuke Nomichi,<sup>†</sup> Masashi Hasegawa,<sup>†</sup> Taku Okada,<sup>‡</sup> Takehiko Yagi,<sup>‡</sup> and Takumi Kikegawa<sup>§</sup>

<sup>†</sup>Department of Materials Science and Engineering, Nagoya University, Furo-cho, Chikusa, Nagoya 464-8603, Japan

<sup>‡</sup>Institute for Solid State Physics, University of Tokyo, Kashiwanoha, Kashiwa, Chiba 277-8581, Japan

<sup>§</sup>Photon Factory, High Energy Accelerator Research Organization, Tsukuba 305-0801, Japan

**ABSTRACT:** The binary skutterudite  $\text{CoP}_3$  has a large void at the body-centered site of each cubic unit cell and is, therefore, called a nonfilled skutterudite. We investigated its room-temperature compression behavior up to 40.4 GPa in helium and argon using a diamond-anvil cell. High-pressure in situ X-ray diffraction and Raman scattering measurements found no phase transition and a stable cubic structure up to the maximum pressure in both media. A fitting of the present pressure–volume data to the third-order Birch–Murnaghan equation of state yields a zero-pressure bulk modulus  $K_0$  of 147(3) GPa [pressure derivative  $K_0'$  of 4.4(2)] and 171(5) GPa [where  $K_0' = 4.2(4)$ ] in helium and argon, respectively. The Grüneisen parameter was determined to be 1.4 from the Raman scattering measurements. Thus,  $\text{CoP}_3$  is stiffer than other binary skutterudites and could therefore be used as a host cage to accommodate large atoms under high pressure without structural collapse.



## 1. INTRODUCTION

Skutterudite structures ( $\text{CoAs}_3$ -type) belonging to the space group  $Im\bar{3}$  consist of corner-shared  $\text{TX}_6$  octahedra ( $T$  = transition metal and  $X$  = pnictogen), leaving a large void at the body-centered site of the cubic unit cell.<sup>1–3</sup> Such a void could accommodate a large atom to afford a filled skutterudite with the general formula  $\text{MT}_4\text{X}_{12}$ .<sup>4,5</sup> Owing to the loose bond between the  $M$  atom and  $\text{TX}_6$  (i.e., rattling effect<sup>6</sup>), filled skutterudites are quite attractive for their potential applications as functional thermoelectric materials.

Under high pressure, the nonbonding atoms are efficiently inserted into the voids of a binary skutterudite, making the high-pressure technique a powerful tool to synthesize novel skutterudite compounds. Takizawa et al.<sup>7</sup> successfully synthesized Si-, Ge-, Sn-, and Pb-filled  $\text{CoSb}_3$  using a large-volume press at a pressure of 5 GPa. From a different viewpoint, the structural stability of binary skutterudites under high pressure is an interesting and important issue in terms of not only the role of the host cage to accommodate large atoms or molecules but also gaining an understanding of the fundamentals behind the stability of open-structured compounds. Therefore, several high-pressure studies have been conducted on binary skutterudites.<sup>8–12</sup>

Recently, an irreversible high-pressure phase transition was observed in  $\text{TSb}_3$  ( $T = \text{Co, Rh, or Ir}$ ) at a pressure greater than 20 GPa at room temperature.<sup>11,12</sup> This novel phase transition in a binary skutterudite was interpreted as being the result of a pressure-induced self-insertion reaction in which the antimony atoms of the framework invade the body-centered site (2a site). However, this transition was observed only for the antimonides,

and it is unclear whether such a self-insertion reaction can occur irrespective of the composition.

$\text{CoP}_3$  crystallizes with the skutterudite structure under ambient conditions<sup>2,5,13</sup> and exhibits a smaller unit cell volume than  $\text{CoSb}_3$ , given that phosphorus has a smaller atomic radius than antimony. In addition, it also exhibits higher electrical conductivity than  $\text{TSb}_3$  ( $T = \text{Co or Ir}$ ).<sup>13–15</sup> Shirotani et al.<sup>9</sup> examined the structural stability of  $\text{CoP}_3$  using a diamond-anvil cell (DAC) and synchrotron radiation and reported that  $\text{CoP}_3$  was structurally stable up to 7 GPa at room temperature in a pressure medium of a methanol–ethanol mixture. However, the reported phase transition in  $\text{TSb}_3$  occurred above 20 GPa, and so further experiments at higher pressures are needed for  $\text{CoP}_3$ .

In the present study, to further widen and deepen our understanding of the phase transition and stability of binary skutterudites, we carried out compression experiments on  $\text{CoP}_3$  up to 40.4 GPa at room temperature using a DAC. The high-pressure behavior of  $\text{CoP}_3$  was examined by high-pressure in situ X-ray diffraction (XRD) and Raman scattering measurements. The compression experiments were carried out under quasi-hydrostatic conditions by using a noble gas as the pressure medium. To the best of our knowledge, there have been no reports on studies that used noble gases as pressure media for binary skutterudite compounds. The use of noble gases afforded reliable data because the solid noble gases are very soft owing to van der Waals binding even after solidification under high pressures and reduce the deviatoric stress in the sample chamber.<sup>16,17</sup> In this

Received: September 19, 2010

Published: March 15, 2011

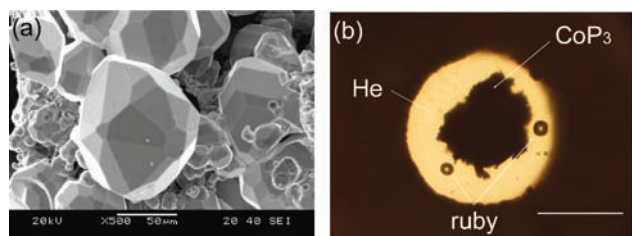


**Figure 1.** (a) SEM image of  $\text{CoP}_3$  single crystals obtained by a tin-flux method at ambient pressure. (b) Photograph of a sample chamber filled with a helium pressure medium at around 1 GPa. The scale bar corresponds to  $100 \mu\text{m}$ .

paper, we discuss the high-pressure behavior of  $\text{CoP}_3$ , including the possibility of noble-gas-filled  $\text{CoP}_3$ .

## 2. EXPERIMENTAL SECTION

A single crystal of  $\text{CoP}_3$  was prepared by the tin-flux method at ambient pressure.<sup>13</sup> This sample was treated with hydrochloric acid to remove the tin, and the obtained products were characterized by scanning electron microscopy together with energy-dispersive spectroscopy (SEM/EDS) and XRD measurements. As shown in the SEM image in Figure 1a, the obtained products exhibited well-habited crystals with sizes on the order of several tens of micrometers. EDS analysis indicated a Co/P composition ratio of 1:2.99 and no detectable amount of tin. This indicates the absence of ternary compounds containing cobalt, phosphorus, and tin. The XRD pattern of the powdered sample indicated  $\text{CoP}_3$  with a very small amount of CoP, which was also detected by EDS analysis at the edges of the  $\text{CoP}_3$  crystals. The measured lattice parameter of  $\text{CoP}_3$  was  $7.7079(5) \text{ \AA}$ , which is consistent with the previously reported value.<sup>2,5,13</sup> In this study, the CoP content was much lower, and, therefore, we crushed these single crystals into a powder for use as the starting material for the high-pressure experiments.

High-pressure experiments were carried out using a DAC with a culet size of  $450 \mu\text{m}$ . A rhenium gasket was precompressed to a thickness of approximately  $100 \mu\text{m}$ , and a sample chamber with a diameter of  $150 \mu\text{m}$  was prepared using a Q-switched YAG laser. The powdered  $\text{CoP}_3$  was carefully placed at the center of the sample hole along with a ruby marker, in order to avoid contact with the gasket. Then, the sample chamber was filled with high-purity helium (>99.99%) or argon (>99.99%) using a modified high-pressure gas loading system.<sup>18</sup> A photograph of the sample chamber immediately after gas loading ( $\sim 1 \text{ GPa}$ ) is shown in Figure 1b. Two runs were made in the present study: Run 1 used helium and  $\text{Mo K}\alpha$  ( $\lambda = 0.7107 \text{ \AA}$ ) radiation from an X-ray source operated at 54 kV and 50 mA at the Institute for Solid State Physics, University of Tokyo, Tokyo, Japan. Run 2 used argon and X-rays from the PF-BL13A synchrotron facility ( $\lambda = 0.4263 \text{ \AA}$ ) at KEK, Tsukuba, Japan. The incident X-rays were directed parallel to the compression axis. The diffracted X-rays were collected using an imaging plate, and the two-dimensional images obtained were integrated into a conventional one-dimensional pattern using the WinPIP code.<sup>19</sup> Unit cell parameters were calculated by the least-squares methods using purpose-built software. A ruby fluorescence method was adopted to determine the pressure, and the same scale was used in both runs.<sup>20</sup> Ruby fluorescence spectra were measured before and after the XRD measurements. In order to evaluate the bulk modulus, the obtained pressure–volume data were fitted to the Birch–Murnaghan equation of state (B–M EOS) as follows:

$$P = \frac{3}{2} K_0 [(V/V_0)^{-7/3} - (V/V_0)^{-5/3}] \left\{ 1 + \frac{3}{4} (K_0' - 4) [(V/V_0)^{-2/3} - 1] \right\}$$

where  $P$ ,  $V_0$ , and  $V$  denote the pressure, the volume at ambient pressure, and the volume at pressure  $P$ , respectively.  $K_0$  and  $K_0'$  are the zero-pressure

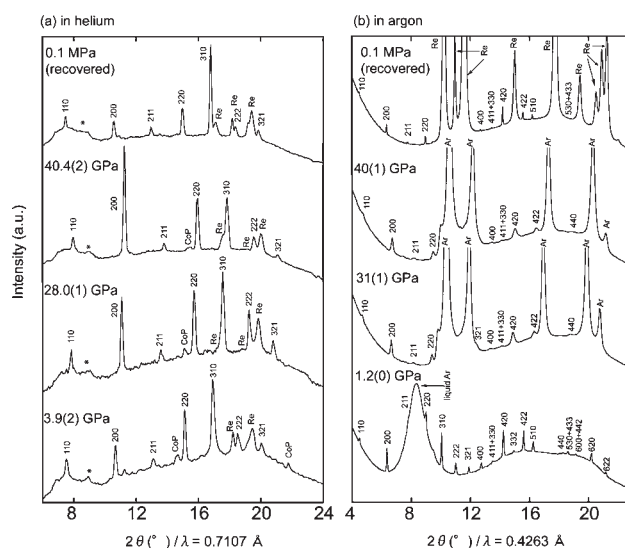


**Figure 2.** XRD profiles of  $\text{CoP}_3$  in helium (a) and argon (b) at high pressures and release of noble gases. Diffraction peaks corresponding to  $\text{CoP}_3$  are labeled with Miller indices. The halo observed in the low- $2\theta$  region in part a might be from the beam stopper or relate to helium.

bulk modulus and its pressure derivative, respectively. If  $K_0'$  is fixed to 4.0, the second-order B–M EOS is obtained.

In run 1, Raman scattering measurements were also carried out during decompression from the highest pressure to ambient pressure at room temperature. An argon-ion laser ( $\lambda = 514.5 \text{ nm}$ , 100 mW) was used as the excitation source and focused to a spot of diameter  $20 \mu\text{m}$  at the sample position through the diamond anvil. The Raman scattering light was dispersed using a grating spectrometer and detected using a liquid- $\text{N}_2$ -cooled charge-coupled device detector. To obtain a high signal-to-noise ratio, the Raman spectrum was recorded over an exposure time of 5 s, and then a total of 20–100 spectra were accumulated after the background was subtracted from each spectrum.

## 3. RESULTS AND DISCUSSION

Parts a and b of Figure 2 show examples of the present XRD profiles for  $\text{CoP}_3$  compressed in helium and argon up to a pressure of approximately 40 GPa at room temperature, respectively. The diffraction peaks could be assigned to the crystalline phases  $\text{CoP}_3$ , CoP, argon, and rhenium (the gasket material). No additional peaks were observed up to the highest pressure in both runs, although the diffraction intensity changed owing to grain rotation caused by deformation of the sample chamber in run 1 and a gradual broadening and weakening of the diffraction peaks in run 2. In Figure 3a, the present data are plotted together with the results of a previous high-pressure experiment<sup>5</sup> in which  $\text{CoP}_3$  was compressed in a methanol–ethanol mixture up to a pressure of 7 GPa at room temperature. The compression curve was extrapolated to higher pressures by using the B–M EOS with  $K_0 = 152(4) \text{ GPa}$  and  $K_0' = 1(1)$  (solid line in Figure 3). As clearly seen from Figure 3a, the pressure–volume curves are consistent with the compression and decompression processes. In addition, no anomalous compression behaviors such as reversible unit cell expansion<sup>21,22</sup> or a self-insertion reaction<sup>11,12</sup> were observed in either pressure media. The XRD measurements indicate that  $\text{CoP}_3$  remained structurally stable and no phase transition occurred. However, in argon,  $\text{CoP}_3$  showed greater broadening of diffraction peaks and less compressibility than in helium. This

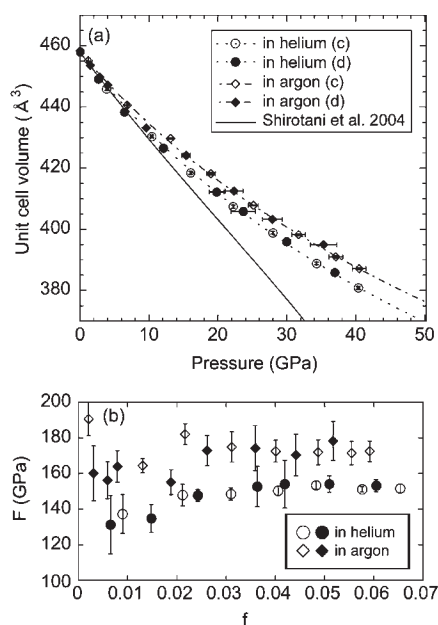


**Figure 3.** (a) Pressure–volume data for  $\text{CoP}_3$  compressed in helium and argon up to a pressure of approximately 40 GPa at room temperature. Circles and diamonds indicate data obtained using helium and argon pressure media, respectively. Solid and open symbols represent the data obtained for compression (denoted as part c) and decompression (denoted as part d), respectively. The dot and dot-dashed lines indicate the equation of state for the present  $\text{CoP}_3$  using helium and argon pressure media, respectively. The solid line indicates the extrapolation of the compression curve reported by Shirovani et al.<sup>9</sup> The Eulerian strain  $f$  dependence of  $F$  is shown in part b. Circles and diamonds correspond to the use of helium and argon, respectively.

might be due to several factors such as the stiffness of solid argon<sup>23</sup> and the location of ruby. Therefore, we limit the discussion of the compression behavior to the results obtained in helium (run 1).

The present pressure–volume data below 10 GPa are in good agreement with the results obtained by Shirovani et al.,<sup>9</sup> whereas those above 10 GPa exhibit much less compressibility than the extrapolation using the EOS. Shirovani et al. obtained a  $K_0$  value of 152(4) GPa and a  $K_0'$  value of 1(1) from the third-order B–M EOS fitting to their pressure–volume data for pressures up to 7 GPa. However, it should be noted that experimental data over a wide pressure range are required when  $K_0'$  is evaluated in a compression experiment. To evaluate  $K_0$  and  $K_0'$ , we examined the normalized pressure ( $F$ ) as a function of the Eulerian strain ( $f$ ) defined as follows:

$$f = [(V/V_0)^{-2/3} - 1]/2$$

$$F = P/[3f(2f + 1)^{5/2}] = K_0 \left[ 1 + \frac{3}{2}(K_0' - 4)f + \dots \right]$$

As shown in Figure 3b, the  $F$ – $f$  plot exhibits a small positive slope. Therefore,  $K_0'$  was obtained with a fitting to the third-order B–M EOS, which yields a  $K_0$  value of 147(3) GPa [ $K_0' = 4.4(2)$ ] and 171(5) GPa [ $K_0' = 4.2(4)$ ] in helium and argon, respectively. Furthermore, the second-order B–M EOS fitting was also made for comparison, which yields a  $K_0$  value of 151.9(6) GPa [ $K_0' = 4.0$  (fixed)] and 172(1) GPa [ $K_0' = 4.0$  (fixed)] in helium and argon, respectively. The  $K_0$  value obtained with the third-order B–M EOS fitting is lower than the value

**Table 1.** Summary of  $K_0$  and  $K_0'$  for Binary Skutterudites Determined by High-Pressure Experiments<sup>a</sup>

	PM	$a$ (Å)	$K_0$ (GPa)	$K_0'$	pressure range
$\text{CoP}_3$	He	7.7079(5)	147(3)	4.4(2)	$P < 40$ GPa <sup>b</sup>
$\text{CoP}_3$	Ar	7.7079(5)	171(5)	4.2(4)	$P < 40$ GPa <sup>b</sup>
$\text{CoP}_3$	He	7.7079(5)	151.9(6)	4.0(fixed)	$P < 40$ GPa <sup>c</sup>
$\text{CoP}_3$	Ar	7.7079(5)	172(1)	4.0(fixed)	$P < 40$ GPa <sup>c</sup>
$\text{CoP}_3$	M–E	7.7064	152(4)	1(1)	$P < 7$ GPa <sup>d</sup>
$\text{CoSb}_3$	M–E	9.0451	81(1)	6(1)	$P < 10$ GPa <sup>d</sup>
$\text{CoSb}_3$	M–E	9.036(5)	93.2(6)	4.0(fixed)	$P < 20$ GPa <sup>e</sup>
$\text{CoSb}_3$	M–E–W	9.036(5)	93(6)	5(1)	$P < 20$ GPa <sup>f</sup>
$\text{CoSb}_3$	M–E	9.0347	84	6.0(fixed)	$P < 10$ GPa <sup>g</sup>
$\text{RhSb}_3$	M–E	9.2255	95	6.0(fixed)	$P < 10$ GPa <sup>g</sup>
$\text{IrSb}_3$	M–E	9.2512(11)	136(5)	4.8(5)	$P < 42$ GPa <sup>h</sup>
$\text{IrSb}_3$	M–E	9.2564	105	6.0(fixed)	$P < 10$ GPa <sup>g</sup>

<sup>a</sup> PM: pressure medium. He: helium. Ar: argon. M–E: methanol–ethanol. M–E–W: methanol–ethanol–water mixture. <sup>b</sup> This study (third-order B–M EOS fitting). <sup>c</sup> This study (second-order B–M EOS fitting). <sup>d</sup> Shirovani et al., 2004. <sup>e</sup> Kraemer et al., 2005. <sup>f</sup> Kraemer et al., 2007. <sup>g</sup> Matsui et al., 2010. <sup>h</sup> Trent et al., 2000.

reported by Shirovani et al. ( $K_0 = 152$  GPa). This might be due to the much larger value of  $K_0'$  (4.4) in this study than in theirs ( $K_0' = 1$ ). Table 1 lists the values of  $K_0$  and  $K_0'$  together with those of other binary skutterudites.

Parts a and b of Figures 4 show the Raman spectra and peak positions for  $\text{CoP}_3$  in helium during decompression from 40.4 GPa to ambient pressure at room temperature. To the best of our knowledge, there have been no reports on the Raman spectrum of  $\text{CoP}_3$  under ambient pressure and the peaks have not yet been identified. Skutterudite has a cubic structure belonging to the space group  $Im\bar{3}$ , with eight active Raman modes ( $\Gamma_R = 2A_g + 2E_g + 4T_g$ ).<sup>24</sup> As shown in Figure 4, we have observed seven sharp peaks (denoted as  $\omega_{1-7}$ ) between 250 and 650  $\text{cm}^{-1}$  at 40.4 GPa, which shifted smoothly toward lower wavenumbers during decompression, with no additional peaks appearing, although the intensity of some peaks changed. In comparison with  $\text{CoSb}_3$ , the Raman peaks of  $\text{CoP}_3$  appeared at higher wavenumbers.<sup>24,25</sup> This might be due to the difference in the lattice parameter and pnictogen mass, as suggested by the previous Raman scattering measurements on filled  $\text{RT}_4\text{Sb}_{12}$  and  $\text{RT}_4\text{P}_{12}$  (R = lanthanides; T = transition metal).<sup>25</sup> The lack of significant change in the Raman spectra is consistent with the XRD results, which indicates that  $\text{CoP}_3$  remains stable up to about 40.4 GPa at room temperature.

The mode Grüneisen parameter ( $\gamma_i$ ) of  $\text{CoP}_3$  can be calculated from the pressure dependence of the Raman frequencies.<sup>26–31</sup> A small sample size is usually required for high-pressure experiments, and it is difficult to measure the Grüneisen parameter by conventional methods under high pressures. Alternatively, Raman scattering measurement is one of the most suitable, convenient, and almost unique methods to obtain directly the vibration mode frequencies of materials under high pressure. In most previous studies using DAC combined with Raman spectroscopy, the mode frequency was fitted to a linear function of pressure and the derivative has been used to obtain  $\gamma_{i,0}$ <sup>26–29</sup>

$$\gamma_{i,0} = K_{T,0}/\omega_{i,0}(\partial\omega_i/\partial P)_{T,0}$$

where  $\omega_i$ ,  $K_{T,0}$ , and  $P$  are the phonon frequency of mode  $i$ , isothermal bulk modulus and pressure, respectively. The subscript

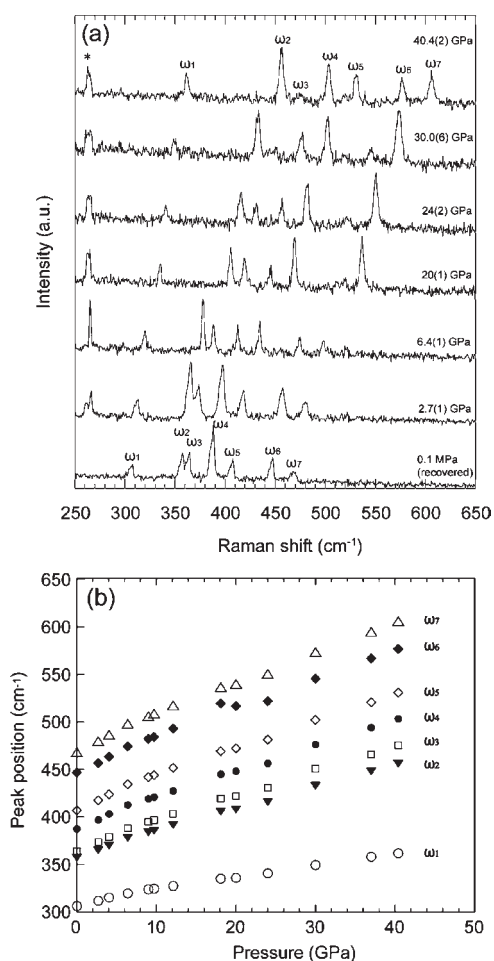


**Figure 4.** (a) Pressure evolution of Raman spectra of CoP<sub>3</sub> in helium for decompression from 40.4 GPa to ambient pressure. Raman peaks from CoP<sub>3</sub>, labeled as  $\omega_i$  ( $i = 1-7$ ). The unshifted peak indicated by an asterisk corresponds to an impurity in the diamond or plasma line of Ar<sup>+</sup>. (b) Pressure dependence of  $\omega_i$  ( $i = 1-7$ ) up to 40.4 GPa.

zero corresponds to the zero-pressure condition. On the other hand, in order to constrain  $\gamma$  from Raman data, a modified procedure has been proposed recently by introducing the following two relations and  $\gamma$  was successfully obtained:<sup>30,31</sup>

$$\gamma_i = -(\partial \ln \omega_i / \partial \ln V)_T$$

$$\gamma_i = \gamma_{i,0}(V/V_0)^q$$

where  $V$  is the unit cell volume calculated from the EOS of CoP<sub>3</sub> and  $q$  is the logarithmic volume derivative of  $\gamma_i$ . This approach avoids some problems<sup>30</sup> and is capable of resulting in an averaged  $\gamma$  over the pressure range of the experiment. In addition, the Raman frequencies of the present CoP<sub>3</sub> show a slight nonlinear pressure dependence, and it causes difficulty in fitting the Raman data by a linear function of pressure. Therefore, we have adopted this procedure to obtain  $\gamma$ . The mode Grüneisen parameter was originally defined as the volume dependence of the vibration mode frequency of the lattice, and it is an important dimensionless number that describes the thermoelastic properties of materials.<sup>32-36</sup> The vibration mode frequencies depend on the element mass, bond strength, coordination environment, and so on. However,  $\gamma$  generally lies between 0.5 and 3 irrespective of the composition.<sup>34</sup>

**Table 2.** Mode Grüneisen Parameters of CoP<sub>3</sub> and Other Binary Skutterudites

$i$	$\omega_{i,0}$ (cm <sup>-1</sup> )	$\gamma_{i,0}$
1	306.27	0.978(9)
2	357.09	1.4(1)
3	363.92	1.54(1)
4	387.37	1.51(1)
5	406.8	1.54(1)
6	446.69	1.48(1)
7	468.13	1.49(1)
	averaged $\gamma_{i,0}$	1.4(2) <sup>a</sup>
		1.49(5) <sup>b</sup>
		ref
CoP <sub>3</sub>		$\gamma = 0.974^c$
CoSb <sub>3</sub>		$\gamma = 1.111^c$
CoSb <sub>3</sub>		$\gamma = 0.952^d$
IrSb <sub>3</sub>		$\gamma = 1.42^e$

<sup>a</sup>This study (using all data). <sup>b</sup>This study (excluding  $i = 1$ ). <sup>c</sup>Shirotani et al., 2004. <sup>d</sup>Caillat et al., 1996. <sup>e</sup>Slack and Tsoukala, 1994.

We fitted the Raman frequencies to the above formula and obtained the mode Grüneisen  $\gamma$  (spectroscopic  $\gamma_{sp}$ ) values ranging from 0.978(9) to 1.54(1) with respect to mode  $i$  ( $q$  was assumed to be unity in the present study for the simplicity in the empirical law<sup>32</sup>). The mode  $i = 1$  might originate from the impurities because this mode frequency exhibited a different volume dependence from that of the others. Table 2 lists the obtained  $\gamma_{sp}$  values together with  $\gamma$  of other binary skutterudites. In comparison, Shirotani et al.<sup>9</sup> reported a  $\gamma$  value of 0.974 for CoP<sub>3</sub>, calculated on the basis of the Debye approximation using the bulk modulus and its pressure derivative (Slater's  $\gamma_{SI}$ <sup>33,34</sup>). We found Slater's  $\gamma_{SI}$  for CoP<sub>3</sub> to be 2.0, which is more than twice their value, by using a  $K_0$  value of 147 GPa and a  $K_0'$  value of 4.4. The discrepancy in  $\gamma_{SI}$  is obviously due to the difference in  $K_0'$ . The present mode Grüneisen parameter for CoP<sub>3</sub> is larger than that reported for CoSb<sub>3</sub> but close to that reported for IrSb<sub>3</sub>, which is stiffer than other antimonide skutterudites. Therefore, the thermoelastic properties of CoP<sub>3</sub> might be similar to those of the p-type semiconductor IrSb<sub>3</sub>.

In the present high-pressure in situ XRD and Raman scattering measurements, no self-insertion reaction was observed in CoP<sub>3</sub> up to 40.4 GPa at room temperature in noble gases. This indicates that CoP<sub>3</sub> with the skutterudite structure is thermodynamically stable up to 40.4 GPa at room temperature and does not form P<sub>x</sub>CoP<sub>3-x</sub>. This behavior is in complete contrast to that of TSb<sub>3</sub>, which transforms into Sb<sub>x</sub>TSb<sub>3-x</sub> above 20 GPa at room temperature. In addition, it must be noted that the large structural void at the body-centered site of the cubic unit cell is comparable in size to the atomic diameters of helium and argon.<sup>37</sup> Therefore, it should be taken into account that noble gases can occupy the voids of CoP<sub>3</sub> under high pressure (i.e., noble-gas-filled CoP<sub>3</sub>). Previous high-pressure studies on open-structured materials found drastic unit cell expansion when the materials were compressed together with noble gas or molecules in the gigapascal pressure range.<sup>21,22</sup> In contrast to these studies, however, no significant expansion of the unit cell was observed in CoP<sub>3</sub> when it was compressed together with helium or argon. However, the possibility of noble-gas-filled CoP<sub>3</sub> remains, especially for helium, because the atomic diameter of helium is much

smaller than that of argon and the size of the voids in CoP<sub>3</sub>. Noble-gas-filled skutterudites are interesting from the viewpoint of phenomena such as the rattling effect, and thus further experimentation using different approaches are required.

#### 4. CONCLUSION

We studied the high-pressure behavior of CoP<sub>3</sub> in helium and argon up to a pressure of 40.4 GPa at room temperature using a DAC combined with high-pressure in situ XRD and Raman scattering measurements. No phase transition was observed in either pressure media, and the cubic structure of CoP<sub>3</sub> was maintained up to a pressure of 40.4 GPa at room temperature. A fitting to the third-order B–M EOS yields  $K_0$  values of 147(3) GPa [ $K_0' = 4.4(2)$ ] and 171(5) GPa [ $K_0' = 4.2(4)$ ] in helium and argon, respectively. The Grüneisen parameter of CoP<sub>3</sub> was determined to be 1.4 from the Raman scattering measurements, and this value is larger than that found in a previous study. CoP<sub>3</sub> is stiffer than other binary skutterudites, making it promising for use as a host cage that can accommodate large atoms or molecules in its voids under very high pressure.

#### AUTHOR INFORMATION

##### Corresponding Author

\*E-mail: niwa@numse.nagoya-u.ac.jp. Tel/Fax: +81-52-789-3253/+81-52-789-3252.

#### ACKNOWLEDGMENT

The authors thank M. Kobashi (Nagoya), O. Terakado (Nagoya), D. Nishio-Hamane (Kashiwa), and H. Gotou (Kashiwa) for their assistance with our experiments. A part of this work was carried out by a joint research at the Institute for Solid State Physics, University of Tokyo, Tokyo, Japan. This research was partially supported by a Grant-in-Aid for Young Scientists (Start-up) and Scientific Researches on Priority Areas from the Ministry of Education, Culture, Sports, Science and Technology of Japan.

#### REFERENCES

- Hulliger, F.; Mooser, E. *Prog. Solid State Chem.* **1965**, *2*, 330–377.
- Ackermann, J.; Wold, A. *J. Phys. Chem. Solids* **1977**, *38*, 1013–1016.
- Schmidt, T. H.; Kliche, G.; Lutz, H. D. *Acta Crystallogr., Sect. C* **1987**, *43*, 1678–1679.
- Jeitschko, W.; Braun, D. *Acta Crystallogr., Sect. B* **1977**, *33*, 3401–3406.
- Jeitschko, W.; Foecker, A. J.; Paschke, D.; Dewalsky, M. V.; Evers, C. B. H.; Künne, B.; Lang, A.; Kotzyba, G.; Rodewald, U. C.; Möller, M. H. *Anorg. Allg. Chem.* **2000**, *626*, 1112–1120.
- Sales, B. C.; Mandrus, D.; Williams, R. K. *Science* **1996**, *272*, 1325–1328.
- Takizawa, H.; Miura, K.; Ito, M.; Suzuki, T.; Endo, T. *J. Alloys Compd.* **1999**, *282*, 79–83.
- Snider, T. S.; Badding, J. V.; Schujman, S. B.; Slack, G. A. *Chem. Mater.* **2000**, *12*, 697–700.
- Shirota, I.; Noro, T.; Hayashi, J.; Sekine, C.; Giri, R.; Kikegawa, K. *J. Phys.: Condens. Matter* **2004**, *16*, 7853–7862.
- Kraemer, A. C.; Perottoni, C. A.; da Jornada, J. A. H. *Solid State Commun.* **2005**, *133*, 173–176.
- Kraemer, A. C.; Gallas, M. R.; da Jornada, J. A. H.; Perottoni, C. A. *Phys. Rev. B* **2007**, *75*, 024105.
- Matsui, K.; Hayashi, J.; Akahira, A.; Ito, K.; Takeda, K.; Sekine, C. *J. Phys.: Conf. Ser.* **2010**, *215*, 012005.
- Watcharapasom, A.; DeMattei, R. C.; Feigelson, R. S.; Caillat, T.; Borshevsky, A.; Snyder, G. J.; Fleurial, J.-P. *J. Appl. Phys.* **1999**, *86*, 6213–6217.
- Slack, G. A.; Tsoukala, V. G. *J. Appl. Phys.* **1994**, *76*, 1665–1671.
- Caillat, T.; Borshevsky, A.; Fleuril, J.-P. *J. Appl. Phys.* **1996**, *80*, 4442–4449.
- Takemura, K. *J. Appl. Phys.* **2001**, *89*, 662–668.
- Klotz, S.; Chervin, J. C.; Munsch, P.; Marchand, G. Le. *J. Phys. D: Appl. Phys.* **2009**, *42*, 075413.
- Yagi, T.; Yusa, H.; Yamakata, M. *Rev. Sci. Instrum.* **1996**, *67*, 2981–2984.
- Fujihisa, H. *Rev. High Pressure Sci. Technol.* **1999**, *9*, 65–70.
- Mao, H. K.; Xu, J.; Bell, P. M. *J. Geophys. Res.* **1986**, *91*, 4673–4676.
- Perottoni, C. A.; da Jornada, J. A. H. *Phys. Rev. Lett.* **1997**, *78*, 2991–2994.
- Yagi, T.; Iida, E.; Hirai, H.; Miyajima, N.; Kikegawa, T.; Bunno, M. *Phys. Rev. B* **2007**, *75*, 174115.
- Mao, H. K.; Badro, J.; Shu, J.; Hemley, R. J.; Singh, A. K. *J. Phys.: Condens. Matter* **2006**, *18*, S963–S968.
- Nolas, G. S.; Kendziora, C. A.; Takizawa, H. *J. Appl. Phys.* **2003**, *94*, 7440–7444.
- Ogita, N.; Kondo, T.; Hasegawa, T.; Takasu, Y.; Udagawa, M.; Takeda, N.; Ishikawa, K.; Sugawara, H.; Kikuchi, D.; Sato, H.; Sekine, C.; Shirota, I. *Physica B* **2006**, *383*, 128–129.
- Gillet, P.; Hemley, R. J.; McMillan, P. F. *Reviews in Mineralogy; Mineralogical Society of America: Washington, DC*, **1998**; Vol. 37, pp 525–590.
- Chopelas, A. *J. Geophys. Res.* **1991**, *96*, 11817–11829.
- Chopelas, A.; Hofmeister, A. M. *Phys. Chem. Miner.* **1991**, *18*, 279–293.
- Gillet, P.; Biellmann, C.; Reynard, B.; McMillan, P. *Phys. Chem. Miner.* **1993**, *20*, 1–18.
- Shim, S. H.; Kubo, A.; Duffy, T. S. *Earth Planet. Sci. Lett.* **2007**, *260*, 166–178.
- Hustoft, J.; Shim, S.-H.; Kubo, A.; Nishiyama, N. *Am. Mineral.* **2008**, *93*, 1654–1658.
- Anderson, O. L. *J. Geophys. Res.* **1979**, *84*, 3537–3542.
- Slater, J. C. *Introduction to Chemical Physics*; McGraw-Hill: New York, **1939**.
- Poirier, J. P. *Introduction to the Physics of the Earth's Interior*, 2nd ed.; Cambridge University Press: Cambridge, U.K., **2000**.
- Barton, M. A.; Stacey, F. D. *Phys. Earth Planet. Inter.* **1985**, *39*, 167–177.
- Vočadlo, N. L.; Price, G. D. *Phys. Earth Planet. Inter.* **1994**, *82*, 261–270.
- Zhang, Y.; Xu, Z. *Am. Mineral.* **1995**, *80*, 670–675.